



THE UNIVERSITY *of* EDINBURGH

Edinburgh Research Explorer

## The importance of ENSO phase during volcanic eruptions for detection and attribution

**Citation for published version:**

Lehner, F, Schurer, AP, Hegerl, GC, Deser, C & Frölicher, TL 2016, 'The importance of ENSO phase during volcanic eruptions for detection and attribution: ENSO phase during volcanic eruptions', *Geophysical Research Letters*, pp. n/a-n/a. <https://doi.org/10.1002/2016GL067935>

**Digital Object Identifier (DOI):**

[10.1002/2016GL067935](https://doi.org/10.1002/2016GL067935)

**Link:**

[Link to publication record in Edinburgh Research Explorer](#)

**Document Version:**

Peer reviewed version

**Published In:**

Geophysical Research Letters

**Publisher Rights Statement:**

©2016. American Geophysical Union. All Rights Reserved.

**General rights**

Copyright for the publications made accessible via the Edinburgh Research Explorer is retained by the author(s) and / or other copyright owners and it is a condition of accessing these publications that users recognise and abide by the legal requirements associated with these rights.

**Take down policy**

The University of Edinburgh has made every reasonable effort to ensure that Edinburgh Research Explorer content complies with UK legislation. If you believe that the public display of this file breaches copyright please contact [openaccess@ed.ac.uk](mailto:openaccess@ed.ac.uk) providing details, and we will remove access to the work immediately and investigate your claim.



## **The importance of ENSO phase during volcanic eruptions for detection and attribution**

**Flavio Lehner<sup>1</sup>, Andrew P. Schurer<sup>2</sup>, Gabriele C. Hegerl<sup>2</sup>, Clara Deser<sup>1</sup>, and Thomas L. Frölicher<sup>3</sup>**

<sup>1</sup>Climate Analysis Section, National Center for Atmospheric Research, Boulder, USA

<sup>2</sup>School of Geosciences, University of Edinburgh, Edinburgh, UK

<sup>3</sup>Environmental Physics, Institute of Biogeochemistry and Pollutant Dynamics, ETH Zürich, Switzerland

Corresponding author: Flavio Lehner ([flehner@ucar.edu](mailto:flehner@ucar.edu))

This article has been accepted for publication and undergone full peer review but has not been through the copyediting, typesetting, pagination and proofreading process which may lead to differences between this version and the Version of Record. Please cite this article as doi: 10.1002/2016GL067935

## Abstract

Comparisons of the observed global-scale cooling following recent volcanic eruptions to that simulated by climate models from the Coupled Model Intercomparison Project 5 (CMIP5) indicate that the models overestimate the magnitude of the global temperature response to volcanic eruptions. Here we show that this overestimation can be explained as a sampling issue, arising because all large eruptions since 1951 coincided with El Niño events, which cause global-scale warming that partially counteracts the volcanically-induced cooling. By subsampling the CMIP5 models according to the observed El Niño Southern Oscillation (ENSO) phase during each eruption, we find that the simulated global temperature response to volcanic forcing is consistent with observations. Volcanic eruptions pose a particular challenge for the detection and attribution methodology, as their surface impacts are short-lived and hence can be confounded by ENSO. Our results imply that detection and attribution studies must carefully consider sampling biases due to internal climate variability.

## Key Points:

- There is disagreement between observed and simulated global-mean cooling response to recent volcanic eruptions
- Accounting for the observed coincidence of El Niño events with recent eruptions resolves this bias
- Detection and attribution studies must consider sampling biases arising from internal variability

Accepted

## 1 Introduction

Detection and attribution is a key tool used for identifying the factors that contribute to observed changes in climate over the past century, and for quantifying the response to individual forcings, such as greenhouse gases, aerosols, or volcanic eruptions (Bindoff et al. 2013; Hasselmann 1993). Estimates of the relative contributions by anthropogenic and natural forcings inform our attempts to constrain transient and equilibrium climate sensitivity (Collins et al. 2013). Yet, such attempts are inherently complicated by the fact that we observe only one of many possible climate trajectories. With internal variability contributing significantly to decadal-scale trends in certain quantities and regions, robust attribution of climate change can become challenging and sensitive to the particular realization of variability sampled in the observational record (Deser et al. 2012a).

Using the CMIP5 (Taylor et al. 2012) multi-model ensemble, studies have estimated the contribution of natural forcing, such as explosive volcanic eruptions and variations in solar irradiance, to the evolution of global mean surface temperature (GMST) since 1951 (Jones et al. 2013; Gillett et al. 2013; Johansson et al. 2015a). Scaling the model simulations to match the observed global mean surface temperature record, these studies concluded that the CMIP5 models as a group overestimate the global temperature response to natural forcing by a factor of two, with uncertainties that render it highly unlikely that the multi-model mean is consistent with the observed record. Since variations in solar irradiance during this time period are small, the models are suspected to produce excessive cooling mainly in response to volcanic eruptions (Bindoff et al. 2013). Paleoclimate model-data comparisons also find that models have a larger volcanic response than suggested by many (Schurer et al. 2013), although not all reconstructions (Hegerl 2003). Large uncertainties remain with these comparisons, including how tree ring data reflect short-term volcanic cooling (Stoffel et al. 2015). Hence the question arises whether climate models systematically overestimate the response to volcanism and what the causes might be.

The sample size used in the evaluation of the models' response to volcanic eruptions is very small, with only three large tropical volcanic eruptions having occurred since 1951: Agung in March 1963, El Chichon in April 1982, and Pinatubo in June 1991. In addition, these three eruptions all coincided with El Niño events, heavily biasing the observed sample towards El Niño as the climate background state (Figure 1). The background climate state can be important for the response of the climate system to an eruption (Ding et al. 2014; Zanchettin et al. 2013; Frölicher et al. 2013). Recent research suggests an increased likelihood for El Niño in the year of or following a volcanic eruption, with a subsequent increased likelihood for La Niña in the year following the El Niño (Adams et al. 2003; McGregor and Timmermann 2011; Li et al. 2013; Lehner et al. 2015; Maher et al. 2015; Chikamoto et al. 2016). Many studies rely at least in part on the dynamical thermostat mechanism to explain this (Clement et al. 1996). However, some modeling studies suggest that the initial tropical Pacific sea surface temperature response to a volcanic eruption resembles La Niña, but the sea surface height response is more indicative of El Niño (McGregor and Timmermann 2011; Maher et al. 2015). It is worth noting that considerable uncertainties exist regarding the chronology of events in the tropical Pacific after an eruption, the dominating processes, and the scalability of these with eruption strength.

In any case, the El Niño events following El Chichon and Pinatubo were already underway before the time of the eruption (Self et al. 1997). Fully coupled simulations and paleoclimate records suggest that the coincidence of El Niño events with three consecutive volcanic eruptions of the same or greater magnitude as Agung, as was the case during 1951-2014, is a very rare occurrence (see Supporting Information Section 1). Also, sampling ENSO

variability itself in coupled climate models requires large ensembles or long control simulations (Wittenberg 2009; Deser et al. 2012b; Stevenson et al. 2012). This issue is exacerbated by volcanic forcing, which causes a GMST response on a similar timescale as ENSO, with tropical Pacific surface temperatures dominating the initial response in GMST. Hence, the effect of volcanic forcing can be confounded by the chance coincidence of an ENSO event (Santer et al. 2001, 2015; Johansson et al. 2015b), something that is not explicitly considered in traditional detection and attribution studies. Linearly removing the ENSO signal from the GMST record (Thompson et al. 2009) would not capture any state dependence or nonlinearity of the response.

El Niño events typically cause positive anomalies in GMST and one might expect that a co-occurrence of El Niño with a volcanic eruption would act to reduce the cooling that arises from the negative radiative forcing of the volcanic aerosols. Here we do not address the question of whether volcanic eruptions cause El Niño events. Rather we investigate the influence of ongoing El Niño events on GMST during the three strong eruptions since 1951. Specifically, we aim to answer the question whether detection and attribution of the influence of natural (volcanic) forcing using CMIP5 models is biased by the unusual realization of ENSO phase during these eruptions. While detection and attribution studies are cautious to interpret results, particularly if based on periods as short as 1951-2010 (Ribes and Terray 2013; Bindoff et al. 2013), the importance of ENSO phase during volcanic eruptions for detection and attribution has not been investigated systematically. To do this, we subsample the model simulations according to ENSO phase and apply simple superposed epoch analysis as well as standard detection and attribution algorithms. The remainder of this paper is structured as follows. Section 2 introduces the data and methods used, Section 3 presents the consequences of the subsampling, and Section 4 summarizes the results and discusses their implications.

## 2 Data and Methods

### 2.1 Observations and model simulations

We use HadCRUT4 (Morice et al. 2012) as surface air temperature observations. Besides HadCRUT4 we also tested other observational datasets (HadCRUT4 infilled (Cowtan and Way 2014), GISTEMP (Hansen et al. 2010), BEST (Rohde et al. 2012), MLOST (Vose et al. 2012)), however, since the results are not dependent on the dataset used (see Figure S1), we do not discuss them further.

We use monthly mean 2-m air temperature from all model simulations with the tag ‘historical’ and ‘historicalNat’ from the CMIP5 archive (see Tables S1, S2, and S3 for details). All model output is bi-linearly regridded to  $5^\circ \times 5^\circ$  and then masked according to where observations exist in the HadCRUT4 data set on a monthly basis.

In addition to CMIP5 we use the 40-member Community Earth System Model (CESM1) Large Ensemble (Kay et al. 2014). The CESM1 Large Ensemble is initiated in 1920 and follows the conventional ‘historical’ forcing protocol of CMIP5. In this ensemble, each member starts from slightly different initial conditions, created by small changes in atmospheric temperature (on the order of  $10^{-14}$  °C).

Finally, we make use of 10-member ‘Pacemaker’ simulations with CESM1. In these simulations the eastern equatorial Pacific sea surface temperature (SST) anomalies are

nudged towards observations (20°S-20°N and 180°W to the American coast), leading to a simulated ENSO evolution in line with observations (as opposed to the free-running simulations of CMIP5 or the CESM1 Large Ensemble, which simulate their own random chronologies of ENSO events). The CESM1 ‘Pacemaker’ ensemble was configured following Kosaka and Xie 2013, using ERSSTv3b for the SST nudging, and starting in 1920.

## 2.2. Subsampling according to ENSO phase

As an indicator of ENSO phase, we use the monthly Nino 3.4 index. We calculate the Nino 3.4 index by averaging the simulated SSTs over the region 170°W-120°W and 5°S-5°N, detrending the resulting time series using a quadratic fit, and then normalizing the detrended Nino 3.4 index. The use of Nino 3 (150°W-90°W, 5°S-5°N) and Nino 4 (160°E-150°W, 5°S-5°N) indices instead of Nino3.4 does not alter our results (not shown).

We consider the three largest volcanic eruptions since 1951: Agung, El Chichon, and Pinatubo. In all cases, an El Niño event (defined when Nino 3.4 index  $> 1\sigma$ ) occurred during the boreal winter (December to February) immediately following the eruption and decayed in the following spring. We subsample the model simulations to mimic this coincidence by considering only simulations that have a Nino 3.4 index  $> 1\sigma$  in any of the months December, January, or February after the eruption start month.

## 3 Results

### 3.1 Average volcanic response

In order to identify the average response of GMST to a major volcanic eruption we conduct a superposed epoch analysis. The GMST response to each volcanic eruption is calculated as anomalies relative to the 5-year average preceding the eruption start date. For CMIP5 we construct the multi-model mean response by averaging across all available simulations. Finally, we average over the three eruptions to get the mean volcanic response.

Figure 2a shows the mean GMST response to the three eruptions (Agung, El Chichon, Pinatubo) in observations and CMIP5. The full CMIP5 multi-model mean suggests an average cooling of  $-0.24\text{ °C}$  [ $-0.39, -0.08$ ; 5-95% range] after an eruption (measured as the first post-eruption minimum in GMST; blue line in Figure 2a). When only those CMIP5 simulations that show an El Niño event during the eruption are selected, the cooling is reduced significantly to  $-0.16\text{ °C}$  [ $-0.42, 0.11$ ] (red line in Figure 2a; 95% significance level), in closer agreement with observations ( $-0.11\text{ °C}$ ; black line in Figure 2a). The timing of the cooling in the subsampled CMIP5 simulations is also in better agreement with observations, with the ongoing El Niño reducing the cooling initially and moderating it over the course of approximately the next two years. Beyond two years, the full and subsampled CMIP5 multi-model means become statistically indistinguishable. The uncertainty range of the subsampled CMIP5 ensemble is larger than that of the full CMIP5 ensemble, since after subsampling fewer simulations go into the multi-model mean and fewer simulations go into the composite of three volcanoes (see Table S1). Note that the observations are noisier than the multi-model mean as they consist of only three samples and can be influenced by a single El Niño event, such as the strong one that occurred in 1982/83 (Figure 1b). Importantly, the 5-95% range of the subsampled CMIP5 simulations encompasses the warming peak from the ongoing El Niño event in observations, while the 5-95% range from the full CMIP5 does not (Figure 2a).

A number of studies have used statistical methods to remove the effects of ENSO and other internal modes of variability from GMST time series (Thompson et al. 2009 and references therein). In Figure 2a the ENSO-adjusted GMST from Thompson et al. 2009 (using HadCRUT3) is shown alongside the raw observational time series. The timing and amplitude of the post-eruption cooling in the adjusted time series is similar to the unconstrained CMIP5 ensemble, indicating that statistical and model-subsampling approaches yield consistent results.

Accepted Article



CMIP5 results may be confounded by the fact that only a subset of models/simulations are sampled when the criterion of the “correct” (same as observed) ENSO phase is applied. Hence, model structural differences are not equally sampled in the two multi-model means. To address this issue, we repeat the analysis with the CESM1 Large Ensemble, thereby ruling out model structural differences (Figure 2b). The full CESM1 ensemble has an average temperature response to volcanic eruptions comparable to the CMIP5 multi-model mean ( $-0.23$  °C [ $-0.32$ ,  $-0.11$ ]). Again, when considering only the simulations with the correct ENSO phase, this response is significantly reduced by about 50% ( $-0.12$  °C [ $-0.36$ ,  $0.08$ ]), in better agreement with observations.

To further investigate whether ENSO phase during an eruption is indeed the dominant factor underlying the improved agreement with observations, we turn to so-called ‘Pacemaker’ simulations with CESM1. These simulations have the observed ENSO phase at all times by design, as the sea surface temperature (SST) anomalies in the eastern equatorial Pacific are nudged towards observations, while elsewhere the coupled model remains unconstrained. Indeed, the 10-member ‘Pacemaker’ ensemble shows a similar evolution as the subsampled CESM1 ensemble as well as good agreement with observations (Figure 2b). However, none of the ‘Pacemaker’ simulations reproduce the magnitude of the observed warming peak 6-9 months after the composite eruption, a feature that is driven primarily by the months following Agung, which saw strong extra-tropical warm anomalies while the El Niño event was only of moderate magnitude (see Figure S7). It is unclear whether these anomalies are at all related to the eruption or the El Niño event. It is possible that 10 ‘Pacemaker’ simulations are not enough to sample the full range of GMST variability. However, we note that adding the eruption of Santa Maria in 1902, another coincidence of a volcanic eruption and an El Niño event, to the observed composite mutes this feature considerably (see Figure S8). Unfortunately, the ‘Pacemaker’ simulations do not include this eruption as they start in 1920.

The uncertainty range for the ‘Pacemaker’ simulations is substantially smaller than for the subsampled CESM1 ensemble, indicating that the ‘Pacemaker’ simulations are more constrained than the subsampled CESM1. This is not surprising given that every ‘Pacemaker’ simulation undergoes the same evolution of tropical Pacific SST anomalies by design, and because tropical Pacific SST anomalies are the leading cause of interannual GMST variability (Stouffer et al. 2000). In the subsampled CESM1 ensemble, on the other hand, different magnitudes and flavors of El Niño can occur that lead to a larger range of temperature responses. However, constraining the ENSO phase in a given model (either via subsampling or nudging) does not guarantee improved agreement with observations, as shown by the results based on the equivalent set of simulations with the Geophysical Fluid Dynamics Laboratory (GFDL) models (see Supporting Information Section 6).

### 3.2 Detection and attribution of volcanic response

Having established the influence of ENSO phase on the GMST response to volcanic eruptions, we turn to the detection and attribution framework in order to estimate the magnitude of the volcanic and anthropogenic fingerprint from observations and investigate if ENSO phase indeed leads to a reduced post-eruption cooling in observations, or whether the discrepancy suggested by the superposed epoch analysis could be due to aliasing an aspect of the forced response.

Detection and attribution performs a multiple regression of the observations onto different forced responses, so-called “fingerprints”, which are here derived from the multi-model mean across simulations subject to natural-only (‘historicalNat’) and natural-and-anthropogenic



forcings ('historical'). The regression is based on a total least-squares approach to account for natural variability (Allen and Stott 2003; Schurer et al. 2013) and estimates a scaling factor  $\beta$  to best match the time-dependent fingerprint  $X_i(t)$  to the observations  $Y(t)$ , taking into account uncertainty in the form of internal variability  $v(t)$  and noise  $v_i$  on the  $i^{\text{th}}$  model fingerprint:

$$Y(t) = \sum_{i=1}^m (X_i(t) - v_i) \beta_i + v(t) \quad (1)$$

Uncertainty ranges for the scaling factors are determined by a Monte-Carlo technique, where random samples of internal variability from the CMIP5 'piControl' simulations are added to an estimate of the (noise-reduced) model fingerprints and observations (Schurer et al. 2013). Here we use globally averaged data as fingerprints, however, our results are very similar to studies that additionally used spatial information (Gillett et al. 2013). The resulting scaling factors determine the magnitude of the forced response to natural forcings only ('historicalNat'), and to natural and anthropogenic forcing combined ('historical'); following from the general form in (1):

$$Y(t) = (X_{\text{historical}}(t) - v_1) \beta_{\text{historical}} + (X_{\text{historicalNat}}(t) - v_2) \beta_{\text{historicalNat}} + v(t) \quad (2)$$

From these values, assuming linearity, we can calculate a scaling factor for the response to anthropogenic forcing ('ANT') and natural forcing ('NAT'),  $\beta_{\text{ANT}}$  and  $\beta_{\text{NAT}}$ , by transforming the scaling factors for historical and historicalNat simulations,  $\beta_{\text{historical}}$  and  $\beta_{\text{historicalNat}}$ , to those for ANT and NAT separately (accounting for the natural forcing within the historical simulation), using the relationship  $X_{\text{historical}}(t) = X_{\text{ANT}}(t) + X_{\text{NAT}}(t)$  (Tett et al. 1999):

$$Y(t) = X_{\text{ANT}}(t) \beta_{\text{historical}} + X_{\text{NAT}}(t) (\beta_{\text{historical}} + \beta_{\text{historicalNat}}) - v_1 \beta_{\text{historical}} - v_2 \beta_{\text{historicalNat}} + v(t) \quad (3)$$

This implies that  $\beta_{historical}$  provides the scaling factor for  $X_{ANT}$ , thus:

$$\beta_{ANT} = \beta_{historical} \quad (4)$$

Finally, the scaling factor for  $X_{NAT}$ ,  $\beta_{NAT}$ , is calculated from  $\beta_{historical}$  and  $\beta_{historicalNat}$  (Section 9 in the Supplementary Information of Tett et al. 1999):

$$\beta_{NAT} = \beta_{historical} + \beta_{historicalNat} \quad (5)$$

Detection and attribution results for continuous time series spanning 1956-2005 (see Figure S2) are very similar to previous studies (e.g., Bindoff et al. 2013; Gillett et al. 2013): the magnitude of the anthropogenic multi-model mean response is detectable in observations (scaling factors which determine the magnitude of the fingerprint are greater than zero,  $p > 0.05$ ; Figure 3a). The range of possible scaling factors encompasses one, suggesting that the amplitude of anthropogenic response in models and observations is consistent. The results for natural forcing, on the other hand, show that the response is detectable but its magnitude is significantly stronger in the models than in the observations by a factor of two (scaling factor of about 0.5; Figure 3a).

In order to test the effect of ENSO phase on our results we repeat the detection and attribution analysis with sub-sampled CMIP5 simulations. Because the number of simulations which are found to have the observed ENSO phase simultaneously for all three eruptions is very small (3 out of 198 ‘historical’ simulations, 0 out of 68 ‘historicalNat’ simulations) we split the time period into three equal 16-year segments with each segment containing one eruption. The time series for each segment then consists of the mean across model simulations with the correct (e.g., observed) ENSO phase (see Figure S2). To keep the number of simulations constant for each segment of the subsampled time series, we restrict the number of simulations to 35 randomly selected ‘historical’ simulations and 13 randomly selected ‘historicalNat’ simulations, the smallest number of available selected simulations across the three eruptions (see Table S1). The final scaling factor ranges are calculated from the combined distribution from 100 such random combinations of available simulations. Detailed analysis shows that splitting the timeseries does not affect the estimated magnitude of the volcanic response (see Supporting Information Section 4 and 5).

Results of the detection and attribution analysis using fingerprints from subsampled simulations yields a scaling factor for natural forcing of about 0.75 with an uncertainty range that encompasses one (Figure 3b). This indicates that the amplitude of the naturally forced response in models is no longer inconsistent with observations and the difference between the model mean and observed response can be explained by internal climate variability.

#### 4 Summary and conclusion

In summary, the GMST response to volcanic eruptions is consistent, within uncertainties, between models and observations when the effects of internal variability, in particular the coincidence of El Niño events (be it by chance or due to an eruption triggering an El Niño event) are explicitly accounted for. This does not rule out that there may be model errors in the response to volcanic eruptions, for example due to errors in the forcing time series itself (Schmidt et al. 2014), due to aerosol-related processes (Stoffel et al. 2015), or due

to the response of the atmospheric circulation to the warming of the stratosphere (Driscoll et al. 2012). Our results have important implications for detection and attribution studies. If a phenomenon under study is rare and the observational record short (as is the case for volcanic eruptions during the 20<sup>th</sup> century), potential superposition of forced and unforced variability needs to be taken carefully into account. These results are also important for paloclimate research, as potential superposition of eruptions and El Niño events during the last millennium adds another source of uncertainty to paleoclimate model-data comparisons (Stoffel et al. 2015, and references therein).

Other aspects of the climate system besides GMST may also be confounded by the superposition of volcanic eruptions and El Niño in the recent past, for example the carbon cycle (Frölicher et al. 2013) and the Southern Annular Mode, which are subject of ongoing research.

## Acknowledgments

We thank John Fasullo, Angeline Pendergrass, Axel Timmermann, and David Paynter for discussion and Tingting Fan and Yu Kosaka for providing the ‘Pacemaker’ simulations (CESM1 and GFDL, respectively). We thank two anonymous reviewers for helpful comments. The National Center for Atmospheric Research is sponsored by the National Science Foundation. FL is supported by an Early Postdoc Mobility fellowship from the Swiss National Science Foundation (SNSF). GH and AS are supported by the ERC funded project TITAN (EC-320691). GH was further supported by NCAS and the Wolfson Foundation and the Royal Society as a Royal Society Wolfson Research Merit Award (WM130060) holder. TLF acknowledges support by the SNSF (Ambizione Grant PZ00PZ-14573). We acknowledge the World Climate Research Programme’s Working Group on Coupled Modelling, which is responsible for CMIP, and we thank the climate modelling groups for producing and making available their model output. For CMIP, the US Department of Energy’s Program for Climate Model Diagnosis and Intercomparison provides coordinating support and led development of software infrastructure in partnership with the Global Organization for Earth System Science Portals. The scripts to generate key figures are provided as supplementary files and the CMIP5 data is available under <https://pcmdi.llnl.gov/projects/esgf-llnl>.

## References

- Adams, B. J., M. E. Mann, and C. M. Ammann, 2003: Proxy evidence for an El Niño-like response to volcanic forcing. *Nature*, **426**, 274–278, doi:10.1038/nature02101.
- Allen, M. R., and P. a. Stott, 2003: Estimating signal amplitudes in optimal fingerprinting, part I: Theory. *Clim. Dyn.*, **21**, 477–491, doi:10.1007/s00382-003-0313-9.
- Bindoff, N., and Coauthors, 2013: Detection and Attribution of Climate Change: from Global to Regional. *Climate Change 2013: The Physical Science Basis. Contribution of Working Group I to the Fifth Assessment Report of the Intergovernmental Panel on Climate Change*.
- Chikamoto, M. O., and Coauthors, 2016: Intensification of tropical Pacific biological productivity due to volcanic eruptions. *Geophys. Res. Lett.*, **43**, doi:10.1002/2015GL067359. <http://doi.wiley.com/10.1002/2015GL067359>.

- Clement, A. C., R. Seager, M. A. Cane, and S. E. Zebiak, 1996: An ocean dynamical thermostat. *J. Clim.*, **9**, 2190–2196, doi:10.1175/1520-0442(1996)009<2190:AODT>2.0.CO;2.
- Collins, M., and Coauthors, 2013: Long-term Climate Change: Projections, Commitments and Irreversibility. *Climate Change 2013: The Physical Science Basis. Contribution of Working Group I to the Fifth Assessment Report of the Intergovernmental Panel on Climate Change*, 1029–1136.
- Cowtan, K., and R. G. Way, 2014: Coverage bias in the HadCRUT4 temperature series and its impact on recent temperature trends. *Q. J. R. Meteorol. Soc.*, n/a – n/a, doi:10.1002/qj.2297. <http://doi.wiley.com/10.1002/qj.2297> (Accessed August 24, 2014).
- Deser, C., R. Knutti, S. Solomon, and A. S. Phillips, 2012a: Communication of the role of natural variability in future North American climate. *Nat. Clim. Chang.*, **2**, 775–779, doi:10.1038/nclimate1562. <http://www.nature.com/doi/10.1038/nclimate1562> (Accessed August 18, 2014).
- , A. Phillips, V. Bourdette, and H. Teng, 2012b: Uncertainty in climate change projections: The role of internal variability. *Clim. Dyn.*, **38**, 527–546, doi:10.1007/s00382-010-0977-x. <http://link.springer.com/10.1007/s00382-010-0977-x> (Accessed July 21, 2014).
- Ding, Y., J. Carton, G. A. Chepurin, G. Stenchikov, A. Robock, L. T. Sentman, and J. P. Krasting, 2014: Ocean response to volcanic eruptions in Coupled Model Intercomparison Project 5 simulations. *J. Geophys. Res.*, 5622–5637, doi:10.1002/2013JC009780. Received. <http://onlinelibrary.wiley.com/doi/10.1002/2013JC009780/full>.
- Driscoll, S., A. Bozzo, L. J. Gray, A. Robock, and G. Stenchikov, 2012: Coupled Model Intercomparison Project 5 (CMIP5) simulations of climate following volcanic eruptions. *J. Geophys. Res. Atmos.*, **117**, 1–45, doi:10.1029/2012JD017607.
- Frölicher, T. L., F. Joos, C. C. Raible, and J. L. Sarmiento, 2013: Atmospheric CO<sub>2</sub> response to volcanic eruptions: The role of ENSO, season, and variability. *Global Biogeochem. Cycles*, **27**, 239–251, doi:10.1002/gbc.20028. <http://doi.wiley.com/10.1002/gbc.20028> (Accessed September 8, 2014).
- Gillett, N. P., V. K. Arora, D. Matthews, and M. R. Allen, 2013: Constraining the ratio of global warming to cumulative CO<sub>2</sub> emissions using CMIP5 simulations. *J. Clim.*, **26**, 6844–6858, doi:10.1175/JCLI-D-12-00476.1.
- Hansen, J., R. Ruedy, M. Sato, and K. Lo, 2010: Global surface temperature change. *Rev. Geophys.*, **48**, doi:10.1029/2010RG000345.
- Hasselmann, K., 1993: Optimal Fingerprints for the Detection of Time-dependent Climate Change. *J. Clim.*, **6**, 1957–1971, doi:10.1175/1520-0442(1993)006<1957:OFFTDO>2.0.CO;2. [http://journals.ametsoc.org/doi/abs/10.1175/1520-0442\(1993\)006%3C1957:OFFTDO%3E2.0.CO;2](http://journals.ametsoc.org/doi/abs/10.1175/1520-0442(1993)006%3C1957:OFFTDO%3E2.0.CO;2) [http://journals.ametsoc.org/doi/pdf/10.1175/1520-0442\(1993\)006%3C1957:OFFTDO%3E2.0.CO;2](http://journals.ametsoc.org/doi/pdf/10.1175/1520-0442(1993)006%3C1957:OFFTDO%3E2.0.CO;2).
- Hegerl, G. C., 2003: Detection of volcanic, solar and greenhouse gas signals in paleo-reconstructions of Northern Hemispheric temperature. *Geophys. Res. Lett.*, **30**, 94–97, doi:10.1029/2002GL016635.
- Johansson, D. J., B. C. O’Neill, C. Tebaldi, and O. Häggström, 2015a: Equilibrium climate sensitivity in light of observations over the warming hiatus. *Nat. Clim. Chang.*, **5**, 449–454, doi:10.1038/nclimate2573. <http://www.nature.com/doi/10.1038/nclimate2573>.
- Johansson, D. J. A., B. C. O’Neill, C. Tebaldi, and O. Häggström, 2015b: Reply to “Volcanic effects on climate.” *Nat. Clim. Chang.*, **6**, 4–5, doi:10.1038/nclimate2861.

- <http://www.nature.com/doi/10.1038/nclimate2861>.
- Jones, G. S., P. a. Stott, and N. Christidis, 2013: Attribution of observed historical near-surface temperature variations to anthropogenic and natural causes using CMIP5 simulations. *J. Geophys. Res. D Atmos.*, **118**, 4001–4024, doi:10.1002/jgrd.50239. <http://doi.wiley.com/10.1002/jgrd.50239> (Accessed September 8, 2014).
- Kay, J. E., and Coauthors, 2014: The Community Earth System Model (CESM) Large Ensemble Project: A Community Resource for Studying Climate Change in the Presence of Internal Climate Variability. *Bull. Am. Meteorol. Soc.*, 141119125353005, doi:10.1175/BAMS-D-13-00255.1. <http://journals.ametsoc.org/doi/abs/10.1175/BAMS-D-13-00255.1>.
- Kosaka, Y., and S.-P. Xie, 2013: Recent global-warming hiatus tied to equatorial Pacific surface cooling. *Nature*, **501**, 403–407, doi:10.1038/nature12534. <http://www.ncbi.nlm.nih.gov/pubmed/23995690> (Accessed July 11, 2014).
- Lehner, F., F. Joos, C. C. Raible, J. Mignot, a. Born, K. M. Keller, and T. F. Stocker, 2015: Climate and carbon cycle dynamics in a CESM simulation from 850 to 2100 CE. *Earth Syst. Dyn.*, **6**, 411–434, doi:10.5194/esd-6-411-2015.
- Li, J., and Coauthors, 2013: El Niño modulations over the past seven centuries. *Nat. Clim. Chang.*, **3**, 822–826, doi:10.1038/nclimate1936. <http://www.nature.com/doi/10.1038/nclimate1936> <http://www.nature.com/nclimate/journal/v3/n9/full/nclimate1936.html>.
- Maher, N., S. McGregor, M. H. England, and A. Sen Gupta, 2015: Effects of volcanism on tropical variability. 1–10, doi:10.1002/2015GL064751.Over.
- McGregor, S., and A. Timmermann, 2011: The effect of explosive tropical volcanism on ENSO. *J. Clim.*, **24**, 2178–2191, doi:10.1175/2010JCLI3990.1.
- Morice, C. P., J. J. Kennedy, N. A. Rayner, and P. D. Jones, 2012: Quantifying uncertainties in global and regional temperature change using an ensemble of observational estimates: The HadCRUT4 data set. *J. Geophys. Res. Atmos.*, **117**, doi:10.1029/2011JD017187.
- Ribes, A., and L. Terray, 2013: Application of regularised optimal fingerprinting to attribution. Part II: Application to global near-surface temperature. *Clim. Dyn.*, **41**, 2837–2853, doi:10.1007/s00382-013-1736-6.
- Rohde, R., R. a Muller, R. Jacobsen, E. Muller, D. Groom, and C. Wickham, 2012: A New Estimate of the Average Earth Surface Land Temperature Spanning 1753 to 2011. *Geoinformatic Geostatistics An Overv.*, **1**, 1–7, doi:<http://dx.doi.org/10.4172/gigs.1000101>.
- Santer, B., S. Solomon, D. Ridley, J. Fyfe, F. Beltran, C. Bonfils, J. Painter, and M. Zelinka, 2015: Volcanic effects on climate. *Nat. Clim. Chang.*, **6**, 3–4, doi:10.1038/nclimate2859. <http://www.nature.com/doi/10.1038/nclimate2859>.
- Santer, B. D., and Coauthors, 2001: Accounting for the effects of volcanoes and ENSO in comparisons of modeled and observed temperature trends. *J. Geophys. Res.*, **106**, 28033, doi:10.1029/2000JD000189.
- Sato, M., J. E. Hansen, M. P. McCormick, and J. B. Pollack, 1993: Stratospheric aerosol optical depths, 1850-1990. *J. Geophys. Res.*, **98**, 22987–22994, doi:10.1029/93JD02553.
- Schmidt, G. a., D. T. Shindell, and K. Tsigaridis, 2014: Reconciling warming trends. *Nat. Geosci.*, **7**, 158–160, doi:10.1038/ngeo2105. <http://www.nature.com/doi/10.1038/ngeo2105>.
- Schurer, A. P., G. C. Hegerl, M. E. Mann, S. F. B. Tett, and S. J. Phipps, 2013: Separating forced from chaotic climate variability over the past millennium. *J. Clim.*, **26**, 6954–6973, doi:10.1175/JCLI-D-12-00826.1.
- Seager, R., S. E. Zebiak, and M. A. Cane, 1988: A Model of the Tropical Pacific Sea Surface Temperature Climatology. *J. Geophys. Res.*, **93**, 1265–1280,



doi:10.1029/JC093iC02p01265.

- Self, S., M. R. Rampino, J. Zhao, and M. G. Katz, 1997: Volcanic aerosol perturbations and strong El Niño events: No general correlation. *Geophys. Res. Lett.*, **24**, 1247, doi:10.1029/97GL01127.
- Stevenson, S., B. Fox-Kemper, M. Jochum, R. Neale, C. Deser, and G. Meehl, 2012: Will There Be a Significant Change to El Niño in the Twenty-First Century? *J. Clim.*, **25**, 2129–2145, doi:10.1175/JCLI-D-11-00252.1.
- Stoffel, M., and Coauthors, 2015: Estimates of volcanic-induced cooling in the Northern Hemisphere over the past 1,500 years. *Nat. Geosci.*, **8**, 784–788, doi:10.1038/ngeo2526. <http://www.nature.com/doi/10.1038/ngeo2526>.
- Stouffer, R. J., G. Hegerl, and S. Tett, 2000: A comparison of surface air temperature variability in three 1000-Yr coupled ocean-atmosphere model integrations. *J. Clim.*, **13**, 513–537, doi:10.1175/1520-0442(2000)013<0513:acosat>2.0.co;2.
- Taylor, K. E., R. J. Stouffer, and G. a. Meehl, 2012: An Overview of CMIP5 and the Experiment Design. *Bull. Am. Meteorol. Soc.*, **93**, 485–498, doi:10.1175/BAMS-D-11-00094.1. <http://journals.ametsoc.org/doi/abs/10.1175/BAMS-D-11-00094.1> (Accessed July 9, 2014).
- Tett, S. F. B., P. A. Stott, M. R. Allen, W. J. Ingram, and J. F. B. Mitchell, 1999: Causes of twentieth-century temperature change near the Earth's surface. *Nature*, **399**, 569–572.
- Thompson, D. W. J., J. M. Wallace, P. D. Jones, and J. J. Kennedy, 2009: Identifying signatures of natural climate variability in time series of global-mean surface temperature: Methodology and insights. *J. Clim.*, **22**, 6120–6141, doi:10.1175/2009JCLI3089.1.
- Vose, R. S., and Coauthors, 2012: NOAA's Merged Land–Ocean Surface Temperature Analysis. *Bull. Am. Meteorol. Soc.*, **93**, 1677–1685, doi:10.1175/BAMS-D-11-00241.1.
- Wittenberg, A. T., 2009: Are historical records sufficient to constrain ENSO simulations? *Geophys. Res. Lett.*, **36**, 1–5, doi:10.1029/2009GL038710.
- Zanchettin, D., O. Bothe, H. F. Graf, S. J. Lorenz, J. Luterbacher, C. Timmreck, and J. H. Jungclaus, 2013: Background conditions influence the decadal climate response to strong volcanic eruptions. *J. Geophys. Res. Atmos.*, **118**, 4090–4106, doi:10.1002/jgrd.50229.

Accepted



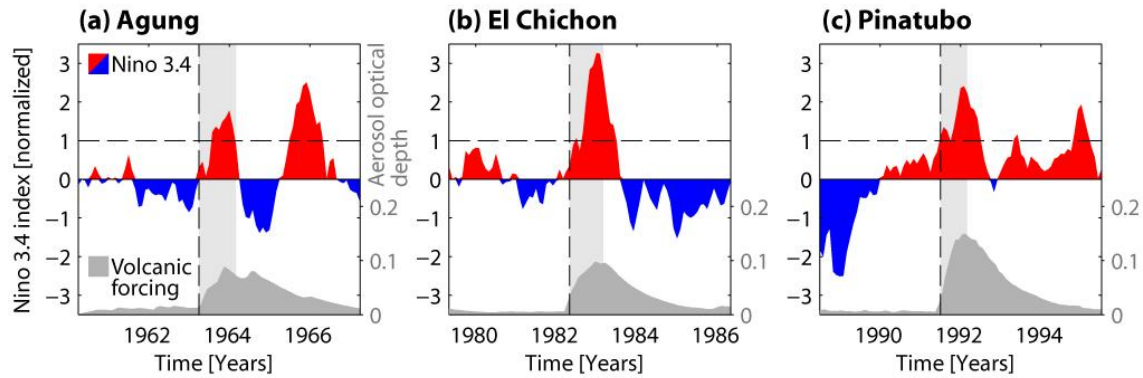


**Figure 1:** Coincidence of volcanic eruptions with El Niño events. Observed Nino 3.4 sea surface temperature anomaly index ([http://www.esrl.noaa.gov/psd/gcos\\_wgsp/Timeseries/Data/nino34.long.anom.data](http://www.esrl.noaa.gov/psd/gcos_wgsp/Timeseries/Data/nino34.long.anom.data); units of standard deviations) and aerosol optical depth (Sato et al. 1993) during the eruptions of (a) Agung, (b) El Chichon, and (c) Pinatubo. Light gray shading indicates the interval between the eruption start date and February of the following year. Horizontal dashed line indicates the El Niño selection criterion (1 standard deviation of the Nino3.4 index).

Accepted

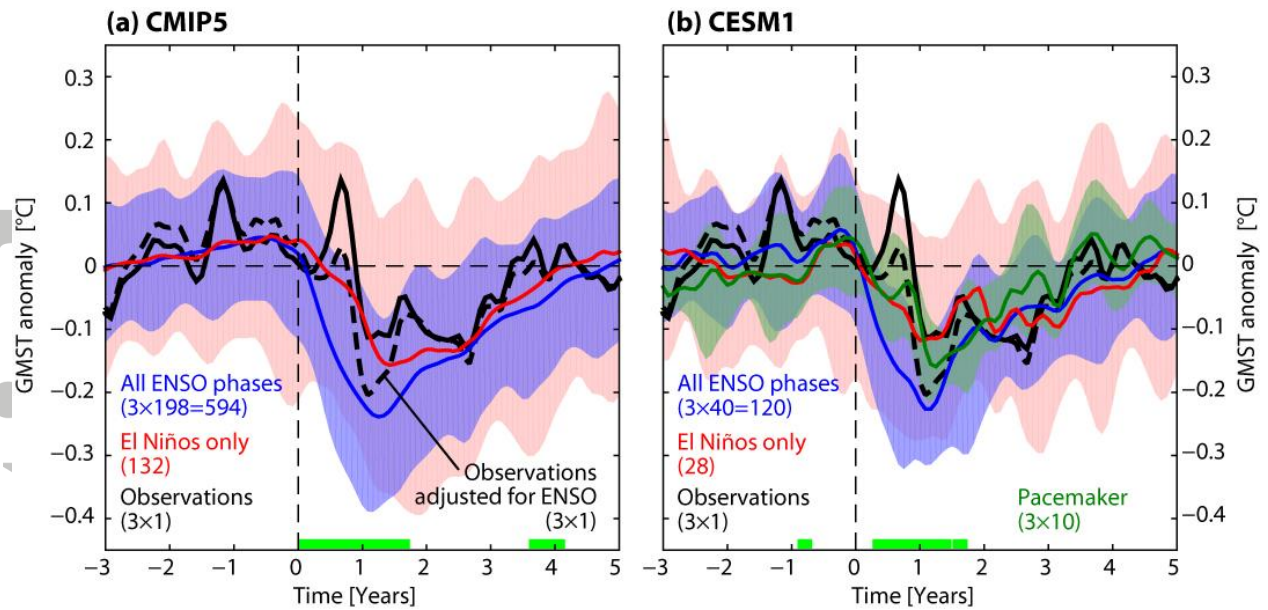


**Figure 2:** Observed and simulated global mean surface temperature (GMST) anomaly relative to the mean of the 5 years preceding the eruption start date (dashed vertical line) averaged over the three recent volcanic eruptions (Agung, El Chichon and Pinatubo). **(a)** CMIP5 historical simulations (all ENSO phases: blue curve and shading; El Niño events only: red curve and shading), and **(b)** CESM1 Large Ensemble (color coding as in (a), and ‘Pacemaker’ simulations (green curve and shading). The solid and dashed black curves show the observations before and after adjusting for the influence of ENSO, respectively – see Thompson et al. 2009. The colored shading gives the 5-95% confidence interval for the model simulations. The months during which the blue and red curves are significantly different (t-test, 95% confidence) are indicated in bright green along the x-axis. The number of ensemble members considered is given in brackets. Time series have been smoothed with a triangular 1-2-1 filter for visual purposes only.

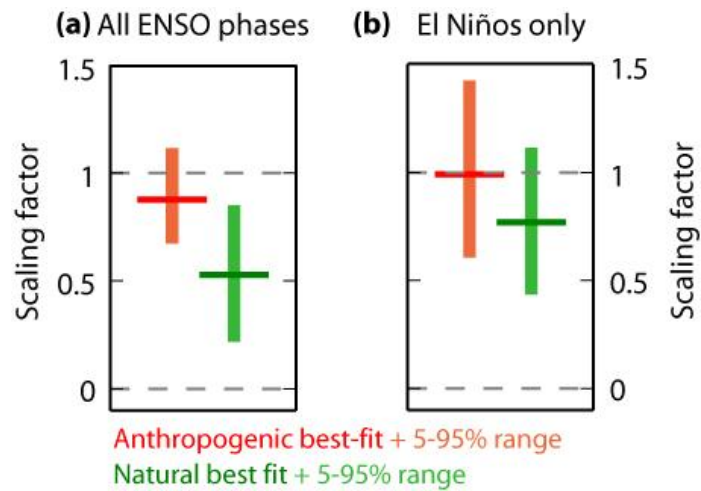


**Figure 3:** Estimated contribution by anthropogenic (red) and natural (green) forcing to global mean surface temperature anomalies from 1956-2005 using **(a)** all CMIP5 simulations and **(b)** only those simulations with the observed ENSO phase. Bold lines are the best-fit scaling factor, shading shows the 5-95% uncertainty range.

Accepted Article